Metal transporter Slc39a10 regulates susceptibility to inflammatory stimuli by controlling macrophage survival

Hong Gao[a,1], Lu Zhao[a,1], Hao Wang[a,b,c], Enjun Xie[a,b], Xinhui Wang[a], Qian Wu[a], Yingying Yu[a], Xuyan He[a], Hongbin Ji[d], Lothar Rink[e], Junxia Min[a,b,2], and Fudi Wang[a,b,c,2]

[a]Department of Nutrition, Nutrition Discovery Innovation Center, Institute of Nutrition and Food Safety, School of Public Health, The First Affiliated Hospital, School of Medicine, Zhejiang University, Hangzhou 310058, China; [b]Institute of Translational Medicine, The Children's Hospital, Collaborative Innovation Center for Diagnosis and Treatment of Infectious Diseases, School of Medicine, Zhejiang University, Hangzhou 310058, China; [c]Department of Nutrition, Precision Nutrition Innovation Center, School of Public Health, Zhengzhou University, Zhengzhou 450001, China; [d]State Key Laboratory of Cell Biology, Chinese Academy of Science Center for Excellence in Molecular Cell Science, Innovation Center for Cell Signaling Network, Institute of Biochemistry and Cell Biology, Shanghai Institute for Biological Sciences, Chinese Academy of Sciences, Shanghai 200031, China; and [e]Institute of Immunology, Faculty of Medicine, RWTH (Rheinisch-Westfälische Technische Hochschule) Aachen University Hospital, D-52074 Aachen, Germany

Edited by Eric P. Skaar, Vanderbilt University Medical Center, Nashville, TN, and accepted by Editorial Board Member Carl F. Nathan November 1, 2017 (received for review May 25, 2017)

Zn plays a key role in controlling macrophage function during an inflammatory event. Cellular Zn homeostasis is regulated by two families of metal transporters, the SLC39A family of importers and the SLC30A family of exporters; however, the precise role of these transporters in maintaining macrophage function is poorly understood. Using macrophage-specific *Slc39a10*-knockout (*Slc39a10*$^{fl/fl}$;*LysM-Cre*$^{+}$) mice, we found that Slc39a10 plays an essential role in macrophage survival by mediating Zn homeostasis in response to LPS stimulation. Compared with *Slc39a10*$^{fl/fl}$ mice, *Slc39a10*$^{fl/fl}$;*LysM-Cre*$^{+}$ mice had significantly lower mortality following LPS stimulation as well as reduced liver damage and lower levels of circulating inflammatory cytokines. Moreover, reduced intracellular Zn concentration in *Slc39a10*$^{fl/fl}$;*LysM-Cre*$^{+}$ macrophages led to the stabilization of p53, which increased apoptosis upon LPS stimulation. Concomitant knockout of *p53* largely rescued the phenotype of *Slc39a10*$^{fl/fl}$;*LysM-Cre*$^{+}$ mice. Finally, the phenotype in *Slc39a10*$^{fl/fl}$;*LysM-Cre*$^{+}$ mice was mimicked in wild-type mice using the Zn chelator TPEN and was reversed with Zn supplementation. Taken together, these results suggest that Slc39a10 plays a role in promoting the survival of macrophages through a Zn/p53-dependent axis in response to inflammatory stimuli.

SLC39A10 | zinc | macrophage | ZIP10 | inflammation

Macrophages play a critical role in innate immunity through three major functions: phagocytosis, antigen presentation, and immunomodulation (1). Interestingly, Zn was recently linked to antimicrobial responses in macrophages (2). In a mouse model of polymicrobial sepsis, Zn supplementation increased the phagocytic capacity of peritoneal macrophages (PMs) for *Escherichia coli* and *Staphylococcus aureus* (3). On the other hand, Zn chelation restricted the growth of specific pathogens such as *Histoplasma capsulatum* (4). In addition, LPS from Gram-negative bacteria reduced intracellular Zn concentrations in mouse dendritic cells, affecting their maturation (5). These findings indicate that Zn homeostasis in macrophages plays an active role in the antimicrobial response.

In mammals, multiple members of the solute-linked carrier 39 (SLC39A, or ZIP) and solute-linked carrier 30 (SLC30A, or ZnT) metal transporter families are essential for the regulation of Zn homeostasis (6–8). Several lines of evidence suggest that some SLC39A/SLC30A transporters participate in immune regulation by regulating intracellular Zn levels; these include Slc39a6 (9), Slc39a10 (7, 8), Slc39a8 (10), and Slc30a5 (11). In human macrophages, LPS up-regulates the expression of SLC39A8, which promotes Zn uptake and negatively regulates proinflammatory responses by inhibiting IKKβ (12) and IL-10 (13). Interestingly, both SLC39A8 and SLC39A14 were recently associated with Mn transport (14–16). Thus, SLC39A and SLC30A transporters may play a role in the inflammatory response by mediating the homeostasis of Zn and/or other metals.

Despite evidence suggesting a link between SLC39A/SLC30A transporters and macrophage function, precisely how these transporters regulate this function remains poorly understood. Here, we systematically measured the expression of Slc39a and Slc30a transporters in mouse bone marrow-derived macrophages (BMDMs) following LPS stimulation. We found that the expression of *Slc39a10* was significantly decreased following LPS stimulation. By generating and functionally characterizing macrophage-specific *Slc39a10*-knockout (*Slc39a10*$^{fl/fl}$;*LysM-Cre*$^{+}$) mice, we found that loss of *Slc39a10* specifically reduces intracellular Zn and increases apoptosis in macrophages in response to inflammatory stimuli.

Results

***SLC39A10* Is Down-Regulated in Macrophages in Response to LPS Stimulation.** First, we mined a previously published dataset of 106 patients with sepsis (Gene Expression Omnibus dataset

Significance

Zn is essential for maintaining the integrity of the immune system, and Zn homeostasis is tightly regulated by two families of ion transporters, SLC39A and SLC30A. Worldwide, an estimated two billion people have Zn deficiency, a condition that can impair immune function and increase susceptibility to a variety of infections. Despite their important roles in health and disease, the molecular mechanisms that underlie Zn transport and Zn homeostasis in macrophages are poorly understood. Here, we report that SLC39A10 plays an essential role in Zn homeostasis in macrophages, regulating the immune response following inflammatory stimuli. Specifically, we identified a role for SLC39A10 in regulating the survival of macrophages via a Zn/p53-dependent axis during the inflammatory response.

Author contributions: H.G., L.Z., L.R., J.M., and F.W. designed research; H.G., H.W., E.X., X.W., Q.W., Y.Y., X.H., and J.M. performed research; H.J. contributed new reagents/analytic tools; L.R., J.M., and F.W. analyzed data; and H.G., L.Z., J.M., and F.W. wrote the paper.

The authors declare no conflict of interest.

This article is a PNAS Direct Submission. E.P.S. is a guest editor invited by the Editorial Board.

[1]H.G. and L.Z. contributed equally to this work.

[2]To whom correspondence may be addressed. Email: junxiamin@zju.edu.cn or fwang@zju.edu.cn.

This article contains supporting information online at www.pnas.org/lookup/suppl/doi:10.1073/pnas.1708018114/-/DCSupplemental.

GSE63042) (17) and compared the expression levels of *SLC39A* and *SLC30A* family members in peripheral blood cells of sepsis survivors ($n = 78$) and nonsurvivors ($n = 28$). As shown in Fig. 1 *A* and *B*, the expression of six transporters in the SLC39A family were significantly decreased in sepsis survivors compared with nonsurvivors, with *SLC39A10* having the greatest reduction (0.519-fold difference). These results suggest that in humans SLC39A10 may play a role in regulating the host response in sepsis and subsequent complications.

Next, we measured the expression levels of mouse *Slc39a* and *Slc30a* genes in BMDMs obtained from wild-type mice treated with LPS (Fig. 1 *C* and *D*). Consistent with patients' data, the expression of *Slc39a10* was significantly down-regulated following LPS stimulation.

Generation of Macrophage-Specific *Slc39a10*-Knockout Mice. Next, to study the function of Slc39a10 in macrophages, we generated macrophage-specific *Slc39a10*-knockout (*Slc39a10$^{fl/fl}$;LysM-Cre^{+}*) mice using Cre recombinase driven by the myeloid cell-specific lysozyme M promoter (LysM-Cre) (Fig. S1). Loss of *Slc39a10* expression was confirmed by a 95% reduction in *Slc39a10* mRNA levels in PMs of *Slc39a10$^{fl/fl}$;LysM-Cre^{+}* mice compared with control (*Slc39a10$^{fl/fl}$*) mice (Fig. 2*A*). We then used inductively coupled plasma mass spectrometry (ICP-MS) to measure the intracellular concentration of various metals in BMDMs obtained from *Slc39a10$^{fl/fl}$;LysM-Cre^{+}* and control mice. Importantly, of the 15 metals examined, only Zn was significantly lower in *Slc39a10$^{fl/fl}$;LysM-Cre^{+}* BMDMs, and the difference between *Slc39a10$^{fl/fl}$;LysM-Cre^{+}* and control BMDMs was even larger following Zn supplementation (Fig. 2*B*). These results support the notion that Slc39a10 transports primarily Zn in mouse macrophages, which is consistent with previous reports that suggested Slc39a10 functions as a Zn importer in various cell types (6–8, 18).

Reduced LPS-Induced Mortality in *Slc39a10$^{fl/fl}$;LysM-Cre^{+}* Mice. Next, we examined the function of Slc39a10 in macrophages in response to LPS. *Slc39a10$^{fl/fl}$;LysM-Cre^{+}* offspring were born at the expected Mendelian ratio and did not develop any overt phenotype during 12 mo of observation under normal conditions. However, when we stimulated *Slc39a10$^{fl/fl}$;LysM-Cre^{+}* and control mice with a combination of LPS and D-galactosamine (19), the *Slc39a10$^{fl/fl}$;LysM-Cre^{+}* mice had significantly higher survival rate

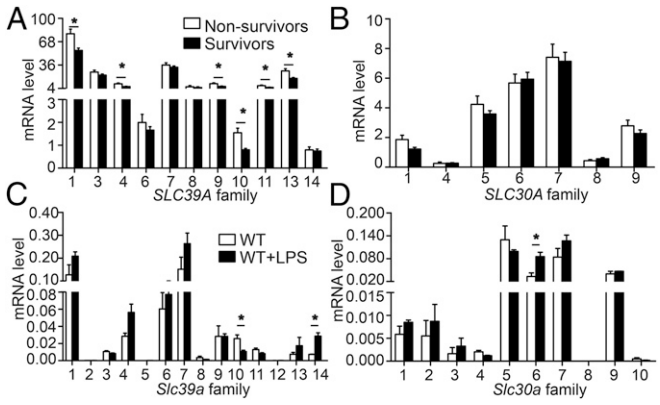

Fig. 1. Summary of *SLC39A* and *SLC30A* gene family expression in human and mouse macrophages. (*A* and *B*) mRNA levels of *SLC39A* (*A*) and *SLC30A* (*B*) genes were measured in both sepsis nonsurvivors ($n = 28$ patients) and survivors ($n = 78$ patients). (*C* and *D*) mRNA levels of *Slc39* (*C*) and *Slc30* (*D*) genes were measured in wild-type mouse BMDMs stimulated with or without LPS ($n = 3$ per group). *$P < 0.05$, Student's *t* test. Detailed information is provided in Table S1.

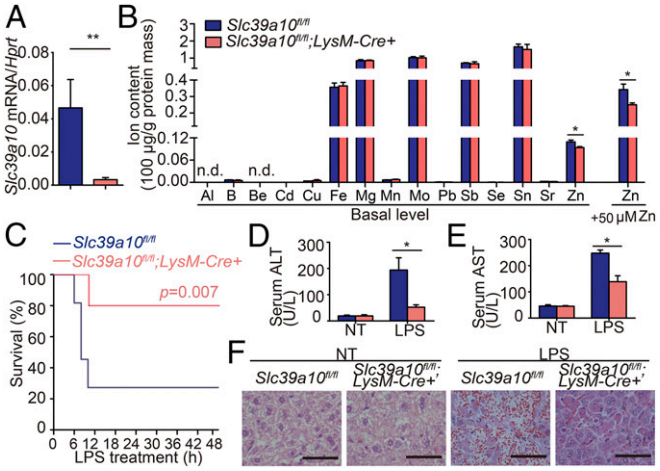

Fig. 2. Macrophage-specific *Slc39a10*-deficient (*Slc39a10$^{fl/fl}$;LysM-Cre^{+}*) mice have improved survival and clinical outcome following LPS stimulation compared with control (*Slc39a10$^{fl/fl}$*) mice. (*A*) *Slc39a10* mRNA was measured in PMs obtained from the indicated mice ($n = 3$ mice per group). (*B*) BMDMs were isolated from *Slc39a10$^{fl/fl}$;LysM-Cre^{+}* and control mice supplemented with or without $ZnCl_2$ (50 μM), and the intracellular concentrations of the indicated metals were measured using ICP-MS ($n = 3$ mice per group). (*C*) Kaplan–Meier survival curve of mice following LPS stimulation ($n = 10$ mice per group). (*D–F*) Serum ALT (*D*), serum AST (*E*), and liver H&E staining (*F*) in the indicated mice either with or without LPS stimulation ($n = 5$). (Scale bars in *F*: 50 μm.) n.d., not detectable; NT, no treatment. *A* and *B* were analyzed by *t* test, *C* by log-rank test, and *D* and *E* by ANOVA. *$P < 0.05$; **$P < 0.01$.

(Fig. 2*C*); specifically, the 12-h survival rate of *Slc39a10$^{fl/fl}$;LysM-Cre^{+}* mice and control mice was 80.0% and 27.3%, respectively.

Upon LPS stimulation, activation of inflammatory molecules can lead to liver damage (20). As expected, 6 h after LPS stimulation, serum alanine transaminase (ALT) and aspartate aminotransferase (AST) levels were increased, and both ALT and AST levels were higher in control mice than in *Slc39a10$^{fl/fl}$;LysM-Cre^{+}* mice (Fig. 2 *D* and *E*). In addition, LPS stimulation led to severe hepatic damage in the control mice but not in the *Slc39a10$^{fl/fl}$;LysM-Cre^{+}* mice (Fig. 2*F*).

Serum, but Not Macrophage, Cytokine Levels Are Significantly Decreased in *Slc39a10$^{fl/fl}$;LysM-Cre^{+}* Mice. Toll-like receptor 4 (TLR4) is the principal receptor for LPS, and activation of TLR4 can increase susceptibility to sepsis, as evidenced by the hyperactivated immune response (the so-called "cytokine storm") that is often responsible for the death of the host. TLR4 signals via both MyD88-dependent and MyD88-independent pathways (21, 22). We therefore measured cytokine levels of both pathways in *Slc39a10$^{fl/fl}$;LysM-Cre^{+}* and control mice. Six hours after LPS stimulation, the levels of major cytokines were significantly reduced in the sera and spleens of *Slc39a10$^{fl/fl}$;LysM-Cre^{+}* mice compared with control mice (Fig. 3 *A* and *B*). These results indicate that the loss of Slc39a10 in macrophages down-regulates cytokine expression, which may explain the resistance of *Slc39a10$^{fl/fl}$;LysM-Cre^{+}* mice to LPS-induced mortality.

We also measured cytokine expression in BMDMs obtained from LPS-stimulated mice. Surprisingly, we found that LPS stimulation induced similar levels of proinflammatory cytokines in the BMDMs of *Slc39a10$^{fl/fl}$;LysM-Cre^{+}* and control mice (Fig. 3 *C* and *D*), suggesting that deleting *Slc39a10* expression in macrophages does not affect their ability to produce these cytokines.

***Slc39a10$^{fl/fl}$;LysM-Cre^{+}* Mice Have Reduced Numbers of Macrophages.** Next, we measured the total number of monocytes in LPS-stimulated *Slc39a10$^{fl/fl}$;LysM-Cre^{+}* and control mice. Interestingly, LPS stimulation reduced the number of monocytes in *Slc39a10$^{fl/fl}$;LysM-Cre^{+}*

BIOCHEMISTRY

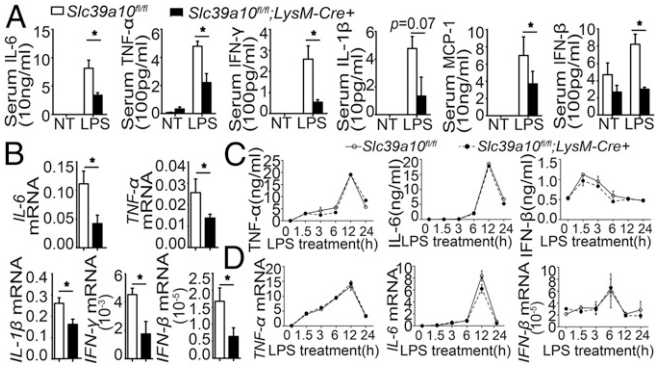

Fig. 3. Cytokine levels in sera, but not in macrophages, are significantly decreased in macrophage-specific *Slc39a10*$^{fl/fl}$;*LysM-Cre*$^{+}$ mice. (*A*) The indicated cytokines levels were measured in the sera of *Slc39a10*$^{fl/fl}$;*LysM-Cre*$^{+}$ and control mice with and without LPS stimulation ($n = 5$ mice per group). (*B*) mRNA levels of the indicated cytokines were measured in the spleen of *Slc39a10*$^{fl/fl}$;*LysM-Cre*$^{+}$ and control mice following LPS stimulation ($n = 5$ mice per group). (*C* and *D*) Protein (*C*) and mRNA (*D*) levels of TNF-α, IL-6, and IFN-β were measured in BMDMs of *Slc39a10*$^{fl/fl}$;*LysM-Cre*$^{+}$ mice and control mice at the indicated times following LPS stimulation ($n = 3$ mice per group). NT, no treatment. *A*, *C*, and *D* were analyzed by ANOVA, *B* by *t* test. $^{*}P < 0.05$.

mice compared with control mice but had no significant effect on the number of neutrophils (Fig. 4*A*), a cell type that also expresses the *LysM* promoter (23). In addition, the percentage of inflammatory macrophages (measured as F4/80^{+} cells) was significantly lower in thioglycollate-elicited PMs and BMDMs from LPS-stimulated *Slc39a10*$^{fl/fl}$;*LysM-Cre*$^{+}$ mice compared with their respective controls (Fig. 4 *B* and *C*). We further examined the affected macrophage subtypes (24, 25) using flow cytometry (Fig. 4*D*) and qPCR (Fig. S2*A*). We found that M1 macrophages were significantly reduced in *Slc39a10*$^{fl/fl}$;*LysM-Cre*$^{+}$ mice, whereas the number of M2 macrophages was unchanged.

Consistent with this finding, immunohistochemistry revealed reduced infiltration of F4/80^{+} macrophages in the spleen and the liver of LPS-treated *Slc39a10*$^{fl/fl}$;*LysM-Cre*$^{+}$ mice (Fig. 4*E*). Moreover, the number of circulating F4/80^{+} macrophages was significantly lower in *Slc39a10*$^{fl/fl}$;*LysM-Cre*$^{+}$ mice than in control mice (Fig. 4*F*). In addition, the number of Ly6C^{+} monocytes, from which inflammatory macrophages are derived (26), was also lower in the bone marrow of *Slc39a10*$^{fl/fl}$;*LysM-Cre*$^{+}$ mice compared with control mice (Fig. 4*F*). Finally, the number of splenic F4/80^{+} macrophages was lower in the *Slc39a10*$^{fl/fl}$;*LysM-Cre*$^{+}$ mice than in control mice (Fig. 4*F*). Taken together, these results suggest that deleting *Slc39a10* expression in macrophages leads to decreased numbers of monocytes and macrophages during the inflammatory response.

LPS Stimulation Induces Macrophage Apoptosis in *Slc39a10*$^{fl/fl}$;*LysM-Cre*$^{+}$ Mice. Next, we investigated the mechanism by which Slc39a10 regulates macrophages by measuring the proliferation and apoptosis of F4/80^{+} macrophages using BrdU incorporation and annexin V/propidium iodide (PI) staining, respectively. We found that the rate of macrophage proliferation was similar in LPS-stimulated *Slc39a10*$^{fl/fl}$;*LysM-Cre*$^{+}$ and LPS-stimulated control mice; however, *Slc39a10*$^{fl/fl}$;*LysM-Cre*$^{+}$ macrophages had a significantly higher level of apoptosis (Fig. 5 *A* and *B*). Moreover, further analyses suggested that this increased apoptosis occurred primarily in M1 macrophages (Fig. S2*B*).

We also measured markers of other types of cell death, including pyroptosis [caspase-1 (27)], necroptosis [MLKL (28)], autophagy [LC3 (29)], and ferroptosis [*Ptgs2* mRNA and lipid peroxidation (30)] in LPS-stimulated *Slc39a10*$^{fl/fl}$;*LysM-Cre*$^{+}$ and control macrophages. As shown in Fig. S3, the levels of these molecular markers were similar in *Slc39a10*$^{fl/fl}$;*LysM-Cre*$^{+}$ and control macrophages. We then examined the effects of specific inhibitors of various types of cell death on the viability of *Slc39a10*$^{fl/fl}$;*LysM-Cre*$^{+}$ macrophages. As shown in Fig. 5*C*, only Z-VAD-FMK, an inhibitor of apoptosis (31), significantly rescued LPS-induced macrophage death; in contrast, inhibitors of necroptosis (necrostatin), autophagy (3-methylademine), and ferroptosis (Ferr-1) (31) had no such effect.

***Slc39a10* Deficiency Does Not Affect Phagocytosis or the *E. coli*-Killing Capacity of Macrophages.** Given that Zn has been reported to affect the phagocytosis of *E. coli* by PMs (3), we examined the phagocytic capacity of *Slc39a10*$^{fl/fl}$;*LysM-Cre*$^{+}$ and control macrophages. However, we found no significant difference with respect to phagocytosis or *E. coli*-killing capacity in *Slc39a10*$^{fl/fl}$;*LysM-Cre*$^{+}$ and control cells (Fig. S4*A*). Because rapid bacterial clearance plays an important role in the host's survival during infection, we also analyzed the survival rates of *Slc39a10*$^{fl/fl}$;*LysM-Cre*$^{+}$ and control mice following *E. coli* infection. Interestingly, the mortality rate was considerably higher in the *Slc39a10*$^{fl/fl}$;*LysM-Cre*$^{+}$ mice (Fig. 5*D*). Further analysis revealed the presence of more *E. coli* cfus in various tissues of *Slc39a10*$^{fl/fl}$;*LysM-Cre*$^{+}$ mice at 12 h after infection (Fig. S4*B*). Collectively, these data suggest that the increased bacterial burden and mortality in *E. coli*-infected *Slc39a10*$^{fl/fl}$;*LysM-Cre*$^{+}$ mice could be attributed to the function of Slc39a10 in controlling the number of macrophages.

p53 Protein Stability Is Increased in the Macrophages of LPS-Stimulated *Slc39a10*$^{fl/fl}$;*LysM-Cre*$^{+}$ Mice. Because p53 is the master transcription factor that controls apoptosis, we measured the expression of p53 in LPS-stimulated *Slc39a10*$^{fl/fl}$;*LysM-Cre*$^{+}$ and LPS-stimulated control mice. Our analysis revealed that p53 protein levels were ~2.6-fold higher in *Slc39a10*$^{fl/fl}$;*LysM-Cre*$^{+}$ macrophages than in control

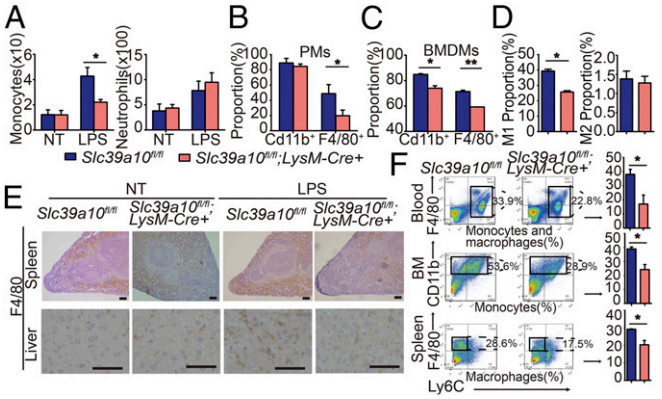

Fig. 4. *Slc39a10*$^{fl/fl}$;*LysM-Cre*$^{+}$ mice have reduced numbers of macrophages. (*A*) Absolute numbers of monocytes and neutrophils were measured in the blood of *Slc39a10*$^{fl/fl}$;*LysM-Cre*$^{+}$ and control mice with and without LPS stimulation ($n = 6$ mice per group). (*B* and *C*) The percentages of CD11b^{+} and F4/80^{+} cells in PMs (*B*) and BMDMs (*C*) were measured in *Slc39a10*$^{fl/fl}$;*LysM-Cre*$^{+}$ and control mice ($n = 3$ mice per group). (*D*) The percentage of peritoneal M1 macrophages (CD11C^{+}F4/80^{+}CD11b^{+}) and M2 macrophages (CD206^{+}F4/80^{+}CD11b^{+}) were measured in LPS-stimulated *Slc39a10*$^{fl/fl}$;*LysM-Cre*$^{+}$ and *Slc39a10*$^{fl/fl}$ mice ($n = 4$ mice per group). (*E*) Immunohistochemical staining for F4/80 in the spleen and liver of *Slc39a10*$^{fl/fl}$;*LysM-Cre*$^{+}$ and control mice with and without LPS stimulation. (Scale bars, 100 μm and 50 μm, respectively.) (*F*) FACS plots (*Left*) and percentages (*Right*) of monocytes and macrophages obtained from the blood, bone marrow (BM), and spleen of *Slc39a10*$^{fl/fl}$;*LysM-Cre*$^{+}$ and control mice following LPS stimulation ($n = 5$ mice per group). NT, no treatment. *A* was analyzed by ANOVA, *B–D* and *F* by *t* test. $^{*}P < 0.05$; $^{**}P < 0.01$.

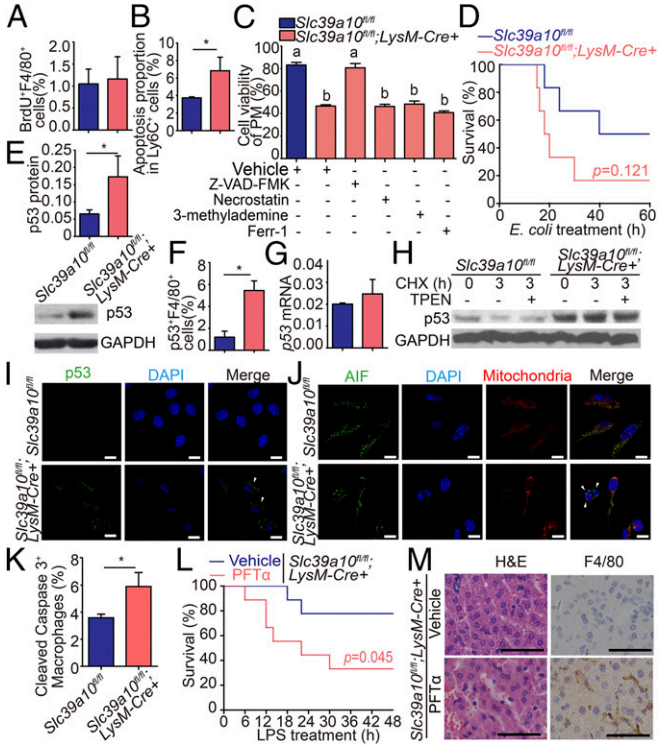

Fig. 5. Increased apoptosis of macrophages in LPS-stimulated *Slc39a10*$^{fl/fl}$;*LysM-Cre*$^{+}$ mice. (*A*) BrdU labeling of splenic macrophages obtained from *Slc39a10*$^{fl/fl}$;*LysM-Cre*$^{+}$ and control mice following LPS stimulation (n = 5 mice per group). (*B*) Annexin-V and PI labeling of apoptotic Ly6C^{+} monocytes in BMDMs obtained from *Slc39a10*$^{fl/fl}$;*LysM-Cre*$^{+}$ and control mice following LPS stimulation (n = 3 mice per group). (*C*) The viability of macrophages treated with inhibitors against apoptosis (Z-VAD-FMK, 10 μM), necroptosis (necrostatin, 10 μg/mL), autophagy (3-methyladenine, 2 mM), and ferroptosis (ferr-1, 10 μM) was measured in LPS-stimulated *Slc39a10*$^{fl/fl}$;*LysM-Cre*$^{+}$ and control mice. (*D*) Kaplan–Meier survival curve of *Slc39a10*$^{fl/fl}$;*LysM-Cre*$^{+}$ and control mice (n = 6 mice per group) following an i.p. injection of *E. coli* (5×10^7 cfu); $P = 0.121$. (*E*) The protein level of p53 in mouse PMs. (*F*) Percentage of circulating p53^{+} F4/80^{+} macrophages (n = 4–5 mice per group). (*G*) The mRNA level of *p53* in mouse PMs (n = 3 mice per group). (*H*) p53 protein levels were measured in PMs before and after 3 h of CHX treatment in the presence and absence of TPEN. (*I*) PMs were isolated from *Slc39a10*$^{fl/fl}$;*LysM-Cre*$^{+}$ and control mice and were immunostained with anti-p53 antibody (green) and DAPI (nucleus, blue). (*J*) PMs were isolated from *Slc39a10*$^{fl/fl}$;*LysM-Cre*$^{+}$ and control mice and were immunostained with anti-AIF antibody (green), MitoTracker dye (mitochondria, red), and DAPI (nucleus, blue). (*K*) Percentage of cleaved caspase-3^{+} macrophages in the mouse spleen (n = 3 mice per group). (*L*) Kaplan–Meier survival curve of vehicle-treated and PFTα-treated *Slc39a10*$^{fl/fl}$;*LysM-Cre*$^{+}$ mice following LPS stimulation (n = 5–7 mice per group). (*M*) H&E and anti-F4/80 immunohistochemical staining of liver sections of LPS-stimulated vehicle-treated or PFTα-treated *Slc39a10*$^{fl/fl}$;*LysM-Cre*$^{+}$ mice. (Scale bars: 10 μm in *I* and *J* and 50 μm in *M*.) *A*, *B*, *E*–*G*, and *K* were analyzed by *t* test, *C* by ANOVA, *D* by log-rank test. *$P < 0.05$. Groups labeled without a common letter were significantly different ($P < 0.05$).

macrophages (Fig. 5*E*); in addition, *Slc39a10*$^{fl/fl}$;*LysM-Cre*$^{+}$ mice contained more p53^{+} macrophages than control mice (Fig. 5*F*). In contrast, the level of *p53* mRNA was similar in LPS-stimulated *Slc39a10*$^{fl/fl}$;*LysM-Cre*$^{+}$ macrophages and LPS-stimulated control macrophages (Fig. 5*G*), suggesting that the difference observed at the protein level was not due to a change in transcription.

Next, we examined the stability of the p53 protein by treating cells with cycloheximide (CHX), an inhibitor of protein synthesis in eukaryotic cells (32). We found higher levels of p53 protein in *Slc39a10*$^{fl/fl}$;*LysM-Cre*$^{+}$ macrophages than in control cells, suggesting that the p53 protein is more stable in *Slc39a10*-deficient macrophages (Fig. 5*H*). Moreover, immunostaining revealed that *Slc39a10*$^{fl/fl}$;*LysM-Cre*$^{+}$ mice have increased numbers of macrophages with pyknotic nuclei and higher levels of cytoplasmic p53 (Fig. 5*I*). In addition, we found that *Slc39a10*$^{fl/fl}$;*LysM-Cre*$^{+}$ macrophages have increased nuclear translocation of apoptosis-inducing factor (AIF) and elevated cleaved caspase-3 levels compared with control macrophages (Fig. 5 *J* and *K*).

p53 Is Required for the Increased Apoptosis of *Slc39a10*$^{fl/fl}$;*LysM-Cre*$^{+}$ Macrophages. Next, we examined the role of p53 in mediating LPS-induced apoptosis of macrophages by treating *Slc39a10*$^{fl/fl}$;*LysM-Cre*$^{+}$ mice with the p53-specific inhibitor pifithrin-α (PFTα) (33). Compared with vehicle-treated *Slc39a10*$^{fl/fl}$;*LysM-Cre*$^{+}$ mice, we found that PFTα-treated *Slc39a10*$^{fl/fl}$;*LysM-Cre*$^{+}$ mice had significantly higher mortality (Fig. 5*L*) as well as increased liver damage and macrophage infiltration (Fig. 5*M*).

To further test the role of p53, we generated macrophage-specific double-knockout (DKO) mice lacking both *p53* and *Slc39a10* expression (*p53*$^{fl/fl}$;*Slc39a10*$^{fl/fl}$;*LysM-Cre*$^{+}$ mice, hereafter referred to as "DKO mice"). Compared with LPS-stimulated *Slc39a10*$^{fl/fl}$;*LysM-Cre*$^{+}$ mice, LPS-stimulated DKO mice had significantly higher mortality (Fig. 6*A*) and more severe liver damage (Fig. 6 *B* and *C*). In addition, following LPS stimulation, the serum levels of several major cytokines were significantly higher in DKO mice than in *Slc39a10*$^{fl/fl}$;*LysM-Cre*$^{+}$ mice (Fig. 6*D*). Moreover, higher percentages of macrophages were detected in DKO BMDMs than in *Slc39a10*$^{fl/fl}$;*LysM-Cre*$^{+}$ BMDMs (Fig. 6*E*), together with increased hepatic macrophages in DKO mice (Fig. 6*F*). Consistent with these findings, our *E. coli* infection model revealed that infected DKO mice have a survival rate and macrophage percentage similar to that of the infected wild-type mice (Fig. S4*C*). Importantly, compared with *Slc39a10*$^{fl/fl}$;*LysM-Cre*$^{+}$ macrophages, DKO macrophages had significantly less apoptosis (Fig. 6*G*). Finally, immunostaining for p53 revealed virtually no detectable p53 or nuclear AIF in DKO macrophages (Fig. 6 *H* and *I*). Taken together, these results suggest that p53 plays a critical role in the improved survival of *Slc39a10*$^{fl/fl}$;*LysM-Cre*$^{+}$ mice following LPS stimulation.

Zn Deficiency in LPS-Stimulated Wild-Type Mice Recapitulates the Phenotype of *Slc39a10*$^{fl/fl}$;*LysM-Cre*$^{+}$ Mice. Finally, we examined whether Slc39a10 affects macrophage survival via intracellular Zn levels. Consistent with our ICP-MS data in BMDMs (Fig. 2*B*), fluozin-3 staining revealed significantly lower levels of Zn in *Slc39a10*$^{fl/fl}$;*LysM-Cre*$^{+}$ PMs than in *Slc39a10*$^{fl/fl}$ cells (Fig. 7*A*). In addition, intracellular Zn was also decreased in *Slc39a10*$^{fl/fl}$;*LysM-Cre*$^{+}$ monocytes but not in *Slc39a10*$^{fl/fl}$;*LysM-Cre*$^{+}$ neutrophils (Fig. S5). The mRNA levels of *Mt1*, a cellular Zn biomarker, were also lower in *Slc39a10*$^{fl/fl}$;*LysM-Cre*$^{+}$ PMs and BMDMs than in *Slc39a10*$^{fl/fl}$ cells (Fig. 7*B*). Moreover, measuring Zn uptake revealed that Zn transport is reduced in *Slc39a10*$^{fl/fl}$;*LysM-Cre*$^{+}$ macrophages compared with *Slc39a10*$^{fl/fl}$ cells (Fig. 7*C*).

Next, we examined the role of Zn on endotoxin resistance in LPS-stimulated *Slc39a10*$^{fl/fl}$;*LysM-Cre*$^{+}$ mice. Notably, following Zn supplementation, *Slc39a10*$^{fl/fl}$;*LysM-Cre*$^{+}$ mice had increased mortality, tissue damage, and liver macrophage infiltration after LPS stimulation compared with vehicle-treated mice (Fig. 7 *D* and *E*).

In contrast, treating wild-type mice with the membrane-permeable Zn-specific chelator TPEN [*N*,*N*,*N*′,*N*′-*tetrakis* (2-pyridylmethyl) ethylenediamine] significantly reduced LPS-induced mortality and liver damage, and these protective effects of TPEN were largely prevented by Zn supplementation (Fig. 7 *F* and *G*). Moreover, TPEN treatment decreased the percentages of Ly6C^{+} monocytes and F4/80^{+} macrophages, and both of these effects were reversed by Zn supplementation (Fig. 7*H*). Furthermore, TPEN increased apoptosis in wild-type BMDMs, and this effect was reversed by Zn supplementation. In contrast, TPEN had little effect on apoptosis in *p53*$^{fl/fl}$;*LysM-Cre*$^{+}$ macrophages (Fig. 7*I*). In addition, TPEN stabilized the p53 protein in both *Slc39a10*$^{fl/fl}$

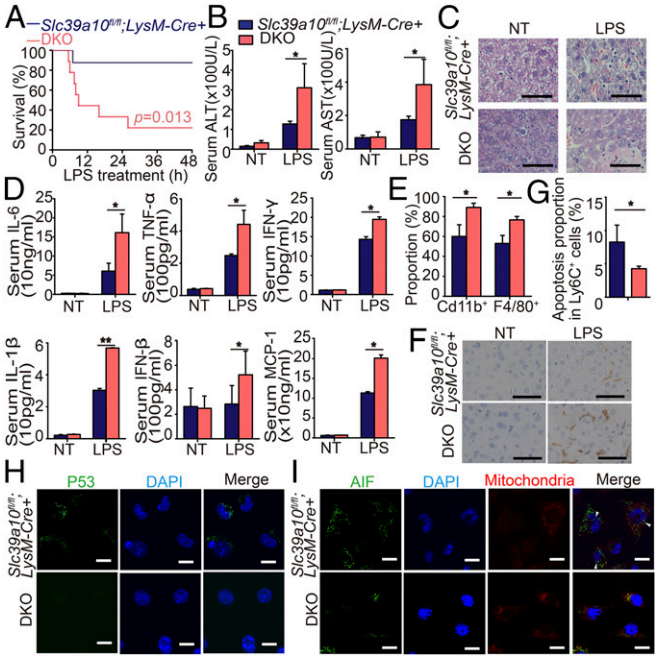

Fig. 6. p53 is required for the improved survival of *Slc39a10*$^{fl/fl}$;*LysM-Cre*$^{+}$ mice following LPS stimulation. (*A*) Kaplan–Meier survival curve of *Slc39a10*$^{fl/fl}$;*LysM-Cre*$^{+}$ and DKO mice following LPS treatment (n = 11 mice per group). (*B*) Serum ALT (*Left*) and AST (*Right*) levels were measured in the indicated mice (n = 5 mice per group). (*C*) Liver H&E staining of the indicated mice. (*D*) The expression of representative cytokines in the serum of *Slc39a10*$^{fl/fl}$;*LysM-Cre*$^{+}$ and DKO mice (n = 5 mice per group). (*E*) The percentage of CD11b^{+} myeloid cells and F4/80^{+} macrophages in BMDMs of *Slc39a10*$^{fl/fl}$;*LysM-Cre*$^{+}$ and DKO mice following LPS stimulation (n = 3 mice per group). (*F*) Anti-F4/80 immunohistochemical staining of liver sections of the indicated mice. (*G*) The percentage of Ly6C^{+} apoptotic monocytes in BMDMs of *Slc39a10*$^{fl/fl}$;*LysM-Cre*$^{+}$ and DKO mice (n = 3 mice per group). (*H*) PMs were isolated from LPS-stimulated *Slc39a10*$^{fl/fl}$;*LysM-Cre*$^{+}$ and DKO mice and were immunostained with anti-p53 antibody (green) and DAPI (nucleus, blue). (*I*) PMs were isolated from LPS-stimulated *Slc39a10*$^{fl/fl}$;*LysM-Cre*$^{+}$ and DKO mice and were immunostained with anti-AIF (green), MitoTracker dye (mitochondria, red), and DAPI (nucleus, blue). (Scale bars: 50 μm in *C* and *F* and 10 μm in *H* and *I*.) NT, no treatment. *A* was analyzed by log-rank test, *B* and *D* by ANOVA, *E* and *G* by *t* test. *P < 0.05; **P < 0.01.

macrophages (Fig. 5*H*) and wild-type macrophages (Fig. S6). Taken together, these results indicate that Slc39a10 modulates LPS-induced apoptosis and endotoxin resistance in macrophages through regulating intracellular Zn homeostasis.

Discussion

Here, we report that the metal transporter SLC39A10 plays an important role in mediating macrophage survival by controlling the cellular import of Zn in a p53-dependent manner. Fukada and coworkers (7, 8) recently reported that Slc39a10 plays a role in B cells. In pro-B cells, loss of Slc30a10 led to increased caspase activity that was accompanied by reduced intracellular Zn, resulting in reduced B cell development (7). In mature B cells, the authors found that Slc39a10 selectively regulates B cell antigen receptor cross-linking and signaling (8). These findings add to our understanding of the role that intracellular Zn plays in immune signaling pathways and highlight the essential function of Slc39a10 in regulating immunity and inflammation.

Zn deficiency is associated with apoptosis in a variety of cell types (34–37), and the viability of both monocytes and macrophages is controlled by a constitutively active process of cell death (38–41). In response to an inflammatory stimulus, the life span of monocytes and macrophages can be extended by inhibiting apoptosis in these cells (41); however, precisely how these dynamic processes underlie the survival and death of macrophages remains unknown. We found that treating mice with a Zn-chelating agent led to increased cell death among monocytes and macrophages as well as up-regulated p53 signaling, in response to LPS stimulation. In our working model (Fig. S7), we propose that SLC39A10-mediated Zn influx in macrophages is essential for maintaining cell survival during the inflammatory response. In the absence of SLC39A10, Zn deficiency leads to the cytoplasmic accumulation of p53 and the nuclear translocation of AIF, which in turn triggers apoptosis.

On the other hand, Zn supplementation can improve the outcome of many infectious diseases, as shown using both animal models and clinical data (2). However, our *Slc39a10*$^{fl/fl}$;*LysM-Cre*$^{+}$ mice have improved survival following LPS stimulation. Moreover, Zn chelation treatment increased survival following LPS stimulation, and this beneficial effect was prevented by Zn supplementation. These seemingly contradictory findings may be attributed to distinct effects of Zn on processes activated by different inflammatory stimuli. Notably, we found that *Slc39a10*$^{fl/fl}$;*LysM-Cre*$^{+}$ mice were more sensitive to *E. coli* infection than *Slc39a10*$^{fl/fl}$ mice; this increased

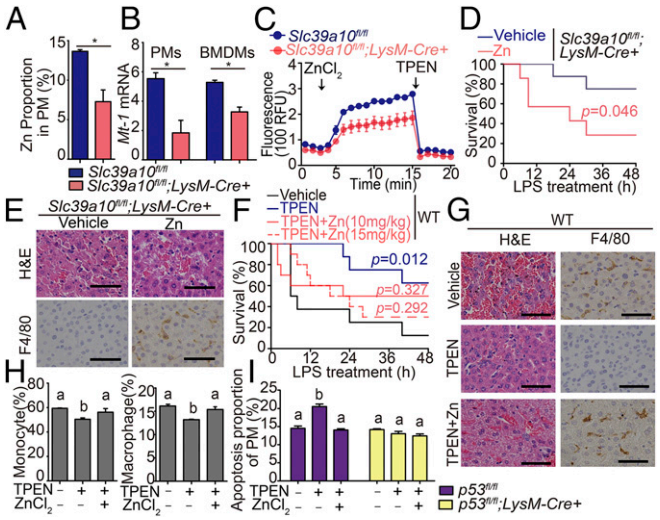

Fig. 7. Zn deficiency induces endotoxin resistance and macrophage apoptosis in LPS-stimulated mice. (*A*) PMs were isolated from *Slc39a10*$^{fl/fl}$;*LysM-Cre*$^{+}$ and *Slc39a10*$^{fl/fl}$ mice, and Zn content was measured using the Zn indicator dye FluoZin-3 (n = 3 mice per group). (*B*) *Mt1* mRNA was measured in PMs and BMDMs isolated from *Slc39a10*$^{fl/fl}$;*LysM-Cre*$^{+}$ and *Slc39a10*$^{fl/fl}$ mice (n = 3 mice per group). (*C*) Intracellular Zn was measured in BMDMs isolated from *Slc39a10*$^{fl/fl}$;*LysM-Cre*$^{+}$ and *Slc39a10*$^{fl/fl}$ mice (n = 3 mice per group). $ZnCl_2$ (60 μM) and TPEN (100 μM) were added at the indicated times. (*D*) Kaplan–Meier survival curve of LPS-stimulated *Slc39a10*$^{fl/fl}$;*LysM-Cre*$^{+}$ mice treated with vehicle or 10 mg/kg Zn (n = 5–7 mice per group). (*E*) H&E and anti-F4/80 staining of liver sections of LPS-stimulated *Slc39a10*$^{fl/fl}$;*LysM-Cre*$^{+}$ mice treated with or without Zn supplementation. (*F*) Kaplan–Meier survival curve of wild-type mice treated with vehicle, TPEN (10 mg/kg), TPEN with 10 mg/kg Zn, and TPEN with 15 mg/kg Zn at LPS stimulation (n = 8–10 mice per group). The survival rates of the TPEN- and/or Zn-treated groups were compared with the vehicle-treated groups, with significance indicated above their respective survival curves. (*G*) H&E and anti-F4/80 staining of liver sections of wild-type mice treated with vehicle, TPEN (10 mg/kg), or TPEN with 10 mg/kg Zn at LPS stimulation. (*H*) The percentage of monocytes and macrophages in BMDMs isolated from wild-type mice treated with vehicle or TPEN (60 μM) with or without Zn (60 μM) (n = 3 mice per group). (*I*) Apoptosis was measured in PMs isolated from LPS-stimulated *p53*$^{fl/fl}$;*LysM-Cre*$^{+}$ mice and *p53*$^{fl/fl}$ mice treated with vehicle or TPEN (60 μM) with or without Zn (60 μM) (n = 3 mice per group). The images in *E* and *G* are representative of ≥3 independent experiments. (Scale bars, 50 μm.) *A* and *B* were analyzed by *t* test, *C*, *H*, and *I* by ANOVA, *D* and *F* by log-rank test. *P < 0.05. Groups labeled without a common letter were significantly different (P < 0.05).

susceptibility is likely due to reduced macrophage numbers and the resulting reduction in total phagocytic capacity. Following bacterial infection, the host's survival requires the rapid clearance of the pathogen by phagocytic cells. Nevertheless, activated macrophages also produce and release large quantities of inflammatory cytokines. Once the immune response is overactivated, it can be detrimental to the host. Our LPS stimulation model recapitulates this immune stage, as inadequate intracellular Zn in *Slc39a10*$^{fl/fl}$;*LysM-Cre*$^{+}$ macrophages led to reduced numbers of stimulated macrophages following LPS exposure, which decreased serum cytokines and helped to protect the liver from subsequent damage.

Given that our macrophage-specific *Slc39a10*-deficient mice have considerable numbers of macrophages that respond to LPS, other Zn transporters are likely to have a compensatory function, thereby fine-tuning the immune response of macrophages during inflammatory stimuli. Future studies should explore the potential role(s) of other Zn transporters in regulating macrophage function and mediating host defense during an inflammatory event.

Materials and Methods

All animal experiments were approved by the Institutional Animal Care and Use Committee of Zhejiang University. The generation of *Slc39a10*$^{fl/fl}$;*LysM-Cre*$^{+}$, *p53*$^{fl/fl}$;*LysM-Cre*$^{+}$, and DKO (*p53*$^{fl/fl}$;*Slc39a10*$^{fl/fl}$;*LysM-Cre*$^{+}$) mice, ICP-MS analysis, and methods used in the collection and culture of primary macrophages, PMs, and BMDMs, fluozin-3 AM staining, immune cell classification, cell-viability assay, phagocytosis, and *E. coli*-killing experiments are presented in *SI Materials and Methods*. Except where indicated otherwise, summary data are expressed as the mean ± SEM. The log-rank test was used to analyze the survival curves, and the Student's *t* test was used to compare two groups. Multiple group comparisons were conducted by one-way ANOVA with Tukey's post hoc test. A P value <0.05 was considered statistically significant.

ACKNOWLEDGMENTS. We thank the members of the F.W. and J.M. laboratories for helpful discussions. This study was supported by National Natural Science Foundation of China Research Grants 31401016 (to L.Z.), 31530034 and 31330036 (to F.W.), 31570791 and 91542205 (to J.M.), 31701035 (to H.W.), and 31701034 (to Q.W.) and Zhejiang Provincial Natural Science Foundation of China Grants LZ15H160002 (to J.M.) and LQ15C110002 (to X.W.).

1. Wynn TA, Chawla A, Pollard JW (2013) Macrophage biology in development, homeostasis and disease. *Nature* 496:445–455.
2. Stafford SL, et al. (2013) Metal ions in macrophage antimicrobial pathways: Emerging roles for zinc and copper. *Biosci Rep* 33:e00049.
3. Nowak JE, Harmon K, Caldwell CC, Wong HR (2012) Prophylactic zinc supplementation reduces bacterial load and improves survival in a murine model of sepsis. *Pediatr Crit Care Med* 13:e323–e329.
4. Winters MS, Chan Q, Caruso JA, Deepe GS, Jr (2010) Metallomic analysis of macrophages infected with Histoplasma capsulatum reveals a fundamental role for zinc in host defenses. *J Infect Dis* 202:1136–1145.
5. Kitamura H, et al. (2006) Toll-like receptor-mediated regulation of zinc homeostasis influences dendritic cell function. *Nat Immunol* 7:971–977.
6. Kaler P, Prasad R (2007) Molecular cloning and functional characterization of novel zinc transporter rZip10 (Slc39a10) involved in zinc uptake across rat renal brush-border membrane. *Am J Physiol Renal Physiol* 292:F217–F229.
7. Miyai T, et al. (2014) Zinc transporter SLC39A10/ZIP10 facilitates antiapoptotic signaling during early B-cell development. *Proc Natl Acad Sci USA* 111:11780–11785.
8. Hojyo S, et al. (2014) Zinc transporter SLC39A10/ZIP10 controls humoral immunity by modulating B-cell receptor signal strength. *Proc Natl Acad Sci USA* 111:11786–11791.
9. Yu M, et al. (2011) Regulation of T cell receptor signaling by activation-induced zinc influx. *J Exp Med* 208:775–785.
10. Aydemir TB, Liuzzi JP, McClellan S, Cousins RJ (2009) Zinc transporter ZIP8 (SLC39A8) and zinc influence IFN-gamma expression in activated human T cells. *J Leukoc Biol* 86:337–348.
11. Nishida K, et al. (2009) Zinc transporter Znt5/Slc30a5 is required for the mast cell-mediated delayed-type allergic reaction but not the immediate-type reaction. *J Exp Med* 206:1351–1364.
12. Liu MJ, et al. (2013) ZIP8 regulates host defense through zinc-mediated inhibition of NF-κB. *Cell Rep* 3:386–400.
13. Pyle CJ, et al. (2017) Zinc modulates endotoxin-induced human macrophage inflammation through ZIP8 induction and C/EBPβ inhibition. *PLoS One* 12:e0169531.
14. Xin Y, et al. (2017) Manganese transporter Slc39a14 deficiency revealed its key role in maintaining manganese homeostasis in mice. *Cell Discov* 3:17025.
15. Lin W, et al. (2017) Hepatic metal ion transporter ZIP8 regulates manganese homeostasis and manganese-dependent enzyme activity. *J Clin Invest* 127:2407–2417.
16. Tuschl K, et al. (2016) Mutations in SLC39A14 disrupt manganese homeostasis and cause childhood-onset parkinsonism-dystonia. *Nat Commun* 7:11601.
17. Tsalik EL, et al. (2014) An integrated transcriptome and expressed variant analysis of sepsis survival and death. *Genome Med* 6:111.
18. Lichten LA, Ryu MS, Guo L, Embury J, Cousins RJ (2011) MTF-1-mediated repression of the zinc transporter Zip10 is alleviated by zinc restriction. *PLoS One* 6:e21526.
19. Lehmann V, Freudenberg MA, Galanos C (1987) Lethal toxicity of lipopolysaccharide and tumor necrosis factor in normal and D-galactosamine-treated mice. *J Exp Med* 165:657–663.
20. Su GL (2002) Lipopolysaccharides in liver injury: Molecular mechanisms of Kupffer cell activation. *Am J Physiol Gastrointest Liver Physiol* 283:G256–G265.
21. Lu YC, Yeh WC, Ohashi PS (2008) LPS/TLR4 signal transduction pathway. *Cytokine* 42:145–151.
22. Kawai T, Akira S (2010) The role of pattern-recognition receptors in innate immunity: Update on toll-like receptors. *Nat Immunol* 11:373–384.
23. Glogauer M, et al. (2003) Rac1 deletion in mouse neutrophils has selective effects on neutrophil functions. *J Immunol* 170:5652–5657.
24. Satoh T, et al. (2010) The Jmjd3-Irf4 axis regulates M2 macrophage polarization and host responses against helminth infection. *Nat Immunol* 11:936–944.
25. Börgeson E, et al. (2015) Lipoxin A4 attenuates obesity-induced adipose inflammation and associated liver and kidney disease. *Cell Metab* 22:125–137.
26. Ginhoux F, Jung S (2014) Monocytes and macrophages: Developmental pathways and tissue homeostasis. *Nat Rev Immunol* 14:392–404.
27. Cerqueira DM, Pereira MS, Silva AL, Cunha LD, Zamboni DS (2015) Caspase-1 but not caspase-11 is required for NLRC4-mediated pyroptosis and restriction of infection by flagellated Legionella species in mouse macrophages and in vivo. *J Immunol* 195:2303–2311.
28. Cai Z, et al. (2014) Plasma membrane translocation of trimerized MLKL protein is required for TNF-induced necroptosis. *Nat Cell Biol* 16:55–65.
29. Huang R, Liu W (2015) Identifying an essential role of nuclear LC3 for autophagy. *Autophagy* 11:852–853.
30. Yang WS, et al. (2014) Regulation of ferroptotic cancer cell death by GPX4. *Cell* 156:317–331.
31. Jiang L, et al. (2015) Ferroptosis as a p53-mediated activity during tumour suppression. *Nature* 520:57–62.
32. Shen J, et al. (2014) Iron metabolism regulates p53 signaling through direct heme-p53 interaction and modulation of p53 localization, stability, and function. *Cell Rep* 7:180–193.
33. Li Y, et al. (2015) A novel dithiocarbamate derivative induces cell apoptosis through p53-dependent intrinsic pathway and suppresses the expression of the E6 oncogene of human papillomavirus 18 in HeLa cells. *Apoptosis* 20:787–795.
34. Reaves SK, et al. (2000) Expression of the p53 tumor suppressor gene is up-regulated by depletion of intracellular zinc in HepG2 cells. *J Nutr* 130:1688–1694.
35. Corniola RS, Tassabehji NM, Hare J, Sharma G, Levenson CW (2008) Zinc deficiency impairs neuronal precursor cell proliferation and induces apoptosis via p53-mediated mechanisms. *Brain Res* 1237:52–61.
36. Ra H, Kim HL, Lee HW, Kim YH (2009) Essential role of p53 in TPEN-induced neuronal apoptosis. *FEBS Lett* 583:1516–1520.
37. Seth R, et al. (2015) Zinc deficiency induces apoptosis via mitochondrial p53- and caspase-dependent pathways in human neuronal precursor cells. *J Trace Elem Med Biol* 30:59–65.
38. Martin KR, Ohayon D, Witko-Sarsat V (2015) Promoting apoptosis of neutrophils and phagocytosis by macrophages: Novel strategies in the resolution of inflammation. *Swiss Med Wkly* 145:w14056.
39. Jaworska J, et al. (2014) NLRX1 prevents mitochondrial induced apoptosis and enhances macrophage antiviral immunity by interacting with influenza virus PB1-F2 protein. *Proc Natl Acad Sci USA* 111:E2110–E2119.
40. Gautier EL, Ivanov S, Lesnik P, Randolph GJ (2013) Local apoptosis mediates clearance of macrophages from resolving inflammation in mice. *Blood* 122:2714–2722.
41. Parihar A, Eubank TD, Doseff AI (2010) Monocytes and macrophages regulate immunity through dynamic networks of survival and cell death. *J Innate Immun* 2:204–215.
42. Kong L, et al. (2009) An essential role for RIG-I in toll-like receptor-stimulated phagocytosis. *Cell Host Microbe* 6:150–161.
43. Zhang Z, et al. (2011) Ferroportin1 deficiency in mouse macrophages impairs iron homeostasis and inflammatory responses. *Blood* 118:1912–1922.